General Hydrodynamic Model for Sewer/Channel Network Systems

By Zhong Ji[1]

Abstract: A general hydrodynamic numerical model for sewer/channel networks is presented. The Priessmann Slot assumption is adopted to extend open channel flow equations to closed conduits under surcharged conditions. The "superlink" algorithm with a staggered grid, implicit scheme is developed to improve the stability and speed of the computation. The SUPERLINK computer model was established without omission of any terms in the St. Venant equations under both subcritical and supercritical flow conditions. The model reduces the order of the sparse matrix equation so that a considerable savings in computational effort is achieved. The numerical experiments show that the model is robust and reliable, and produces consistent results under different grid setups. The application to a large looped sewer network shows a reasonable agreement with field measurement. A comparison between the results from the SUPERLINK and the SWMM EXTRAN model demonstrates that while maintaining the computational stability and accuracy, the computation can be sped up using the SUPERLINK algorithm for the sewer network system, which experienced a wide variety of hydrodynamic conditions.

INTRODUCTION

Mathematical models play a major role in designing and improving storm water collection systems. Simulation results are widely used for planning, designing, and operational purposes. Stability, speed, size, and accuracy of the models for sewer/channel networks, however, are major concerns in current engineering practice.

There are basically two types of numerical schemes for solving the complete unsteady flow equations: explicit and implicit. Explicit schemes are simple and can be easily used to formulate a general network model for sewer/channel systems. The explicit schemes, however, require a small time step and a minimum pipe length, as imposed by the Courant criterion. This limits the computational speed of models using explicit schemes.

Due to the limitations of the explicit schemes, many models have been developed in recent years using implicit schemes (Amein 1968; Fread 1973; Strelkoff 1973; Price 1974; Joliffe 1984; Nguyen and Kawano 1995). The research indicates that implicit schemes are mathematically more sophisticated in formulating a looped network. A four-point implicit scheme, also called the Preissmann Box Scheme, is usually adopted. The scheme results in a sparse matrix equation for the complete unsteady flow equations. The equations are then solved implicitly for flows and depths throughout a network system over a time step based on sewer/channel network connectivity and boundary conditions.

The objective of the present paper is to introduce a discretization scheme for the complete unsteady flow equations, and an algorithm for solving these equations for sewer/channel networks under both free surface and surcharged conditions. The details of the scheme and the algorithm are described. A computer model, SUPERLINK, was developed using the scheme and the algorithm. Numerical experiments were carried out to evaluate the stability, accuracy, and speed of the scheme and the algorithm. Verification was conducted by applying the model to a large looped sewer system. The simulation result is compared with field measurements as well as the SWMM EXTRAN model (Roesner et al. 1988) simulation results.

[1]Hydr. Specialist, Natural Resour. Dept., Wastewater Treatment Div., King County, MS 81, 821 Second Ave., Seattle, WA 98104-1598.

Note. Discussion open until August 1, 1998. To extend the closing date one month, a written request must be filed with the ASCE Manager of Journals. The manuscript for this paper was submitted for review and possible publication on December 4, 1995. This paper is part of the ***Journal of Hydraulic Engineering***, Vol. 124, No. 3, March, 1998. ©ASCE, ISSN 0733-9429/98/0003-0307–0315/$4.00 + $.50 per page. Paper No. 12146.

THEORY AND ASSUMPTIONS

The complete unsteady flow equations for one-dimensional flow under free-surface conditions are used to describe the flow through a sewer/channel system. These equations are a pair of nonlinear partial differential equations: a continuity equation and a momentum equation. The continuity equation describes the mass balance of flow; the momentum equation describes the force balance under dynamic conditions

$$\frac{\partial A}{\partial t} + \frac{\partial Q}{\partial x} = q_0 \tag{1}$$

$$\frac{\partial Q}{\partial t} + \frac{\partial}{\partial x}(Qu) + gA\left(\frac{\partial h}{\partial x} - S_0 + S_f + S_L\right) = 0 \tag{2}$$

where Q = discharge; A = flow cross-sectional area; h = depth; u = velocity; S_0 = bed slope of channel or conduit; S_f = friction head loss slope; S_L = local head loss slope; q_0 = lateral flow over unit length of channel or conduit; g = gravitational acceleration; x = distance; and t = time.

The head loss slope has two components: the frictional head loss slope, S_f, and the local head loss slope, S_L. The friction slope represents the head loss from the shear applied to the wetted perimeter along the longitudinal direction. The local head loss slope represents the energy loss from a sudden change of the flow cross section over a short distance.

Solution of the two partial differential equations requires specification of boundary conditions. The boundary conditions of a system are defined as a stage hydrograph or a rating curve between the flow and stage. Lateral flow to a junction is not considered as a boundary condition in the computation, since the flow is already included in the continuity equation. Stage at a boundary junction governs the depth at the end of the boundary conduit when the stage is relatively high (backwater effect). Depth at the end of the conduit is the lesser of the critical depth and the normal depth when the end conduit experiences a free outfall condition.

A few assumptions are made in solving the flow equations for a sewer system. A fictitious Priessmann Slot (Abbot 1982) is introduced to extend the applicability of the one-dimensional unsteady free-surface flow equations to surcharged conditions in closed conduits. The concept is modified so that only the top width of the slot is used in the computation, and that no extra area and wetted perimeter from the slot are introduced. The width of the slot in the present model is assumed to be 0.1% of the maximum width of a conduit under surcharging conditions, as shown in Fig. 1.

Flooding is considered to occur when a system is over-

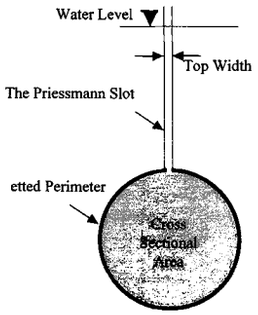

FIG. 1. Schematic of Priessmann Slot

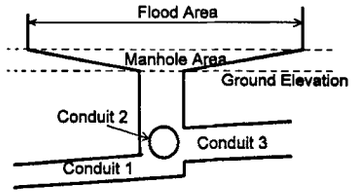

FIG. 2. Setup of Manhole in Computation

loaded. A flood area is assumed on top of a manhole above the ground elevation. Fig. 2 shows the assumed surface area of a manhole at different elevations for computational purposes. Immediately above the ground surface, a smooth transition is introduced between the manhole area and the flood area. A transition depth of 0.5 m is selected in the present model. The specific width of the Priessmann Slot and the flood area are used only for test purposes in this paper and can be adjusted based on the network systems to be examined.

METHODOLOGY

General

Before describing the mathematical formulations for the SUPERLINK model, the concepts of link, node, superlink, and superjunction are introduced to facilitate interpretation. A link can be either a conduit or a section of an open channel. In the present numerical approach, a link is a basic finite volume, and its length is treated as Δx in the numerical computation. A node can be a manhole, a location where the size or slope of the pipe changes, or purely a computational point to segment a conduit when higher resolution of the computational results is desired. A superlink is defined as a collection of links connected end to end at nodes without branching. The ends of superlinks are defined as superjunctions. A superjunction can be a storage junction, a node with one link connected, a node with more than two links connected, or a node attached to a system boundary. A superjunction can also be a node attached to two links with a noticeable difference in invert elevations.

The discretization of the complete unsteady flow equations is the foundation of getting stable and accurate numerical solutions under a wide variety of physical conditions experienced in sewer/channel network systems. The staggered grid scheme, which is conceptually different from the popularly used four-point scheme, is formulated for solving the completely unsteady flow equations. In establishing the numerical scheme, the physical phenomenon of one-dimensional unsteady flow should be described by the discretized continuity and momentum equations as closely as possible. The momentum equation describes the dynamic force balance in the space dimension. The movement of water volume in a link is driven by the force governed mainly by the difference between the head at two end nodes of the link. It is reasonable to apply the momentum equation to a link and solve the flow through the link based on the head at the two end nodes. On the other

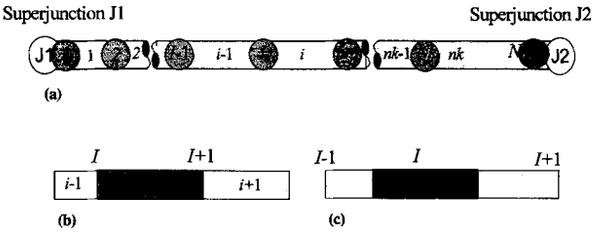

FIG. 3. Staggered Grid Setup of Discretized Superlink: (a) Setup of Staggered Grid in Superlink *k*; (b) Control Volume for Link *i*; (c) Control Volume for Node *I*

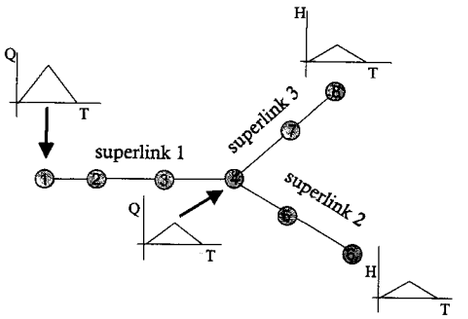

FIG. 4. Sample Sewer Network System

hand, to find the flow at a node can be confusing when lateral flow is applied to a manhole. The continuity equation should be applied around the node rather than a link to avoid this confusion. With the prior considerations, it is physically more appropriate to apply the continuity and momentum equations in a series of staggered control volumes in the computational domain rather than to find flow and head at the same locations, as suggested by the four-point scheme. Applying the staggered grid and implicit scheme to a superlink (e.g., superlink *k*) with *nk* links, the depth is solved at *nk*-1 nodes, and the flow is solved in *nk* links subject to the heads at two ends of the superlink. The schematic of the staggered grid is shown in Fig. 3(a).

The superlink algorithm with the staggered grid implicit scheme is derived in two steps for the solution, as discussed in detail in the following sections. The first step is to derive the recurrence relations according to the discretized continuity equation and the momentum equation for each superlink using the staggered grid implicit scheme. The definition of the superlink facilitates the derivation, since there will be no off-diagonal nonzero elements in the coefficient matrix formulated for one superlink. A series of superlink recurrence relations relating flows and depths in the links and nodes of each superlink can be derived (see Appendix I for details). A condensed sparse matrix is created in the second step of the development by applying the continuity equation to all superjunctions in the system using the recurrence relations for each superlink developed in the first step. The order of the matrix set up in this way is equal to the number of superjunctions in the system instead of twice the number of nodes in the system, as is the case in other implicit schemes directly discretized from the complete unsteady flow equations. This order reduction of the matrix facilitates the solution procedure and speeds up the computation.

A simple network system in Fig. 4 is used as an example to illustrate the advantage of the superlink algorithm with the staggered grid implicit scheme in sparse matrix formation. The sparse matrix equation formulated based on the superlink algorithm with the staggered grid implicit scheme is expressed as

$$
\begin{bmatrix} * & * & & \\ * & * & * & * \\ & & * & \\ & & & * \end{bmatrix}
\begin{bmatrix} H_1^{t+\Delta t} \\ H_4^{t+\Delta t} \\ H_6^{t+\Delta t} \\ H_8^{t+\Delta t} \end{bmatrix}
=
\begin{bmatrix} RHS_1 \\ RHS_2 \\ RHS_3 \\ RHS_4 \end{bmatrix} \tag{3}
$$

where "$*$" indicates corresponding nonzero coefficient; and RHS_i = right-hand side of eq. i. The same network may be expressed as the following sparse matrix equation based on directly discretizing the continuity and the momentum equations using the four-point implicit scheme:

$$
\left[\begin{array}{cccccccccccccccccc}
* & * & * & * \\
* & * & * & * \\
& & * & * & * & * \\
& & * & * & * & * \\
& & & & * & * & * & * \\
& & & & * & * & * & * \\
& & & & & & * & * & * & * \\
& & & & * & * & * & * \\
& & & & & & * & & * & & * & * \\
& & & & & & * & & & * & & & & & * & * \\
& & & & & & * & & * & & * & * \\
& & & & & & * & & * & & * & * \\
& & & & & & & & & & * & * & * & * \\
& & & & & & & & & & * & * & * & * \\
& & & & & & * & & & * & & & & & * & * \\
& & & & & & * & & & * & & & & & * & * \\
& & & & & & & & & & & & & & * & * & * & * \\
& & & & & & & & & & & & & & * & * & * & *
\end{array}\right]
\begin{bmatrix} \Delta H_1 \\ \Delta Q_1 \\ \Delta H_2 \\ \Delta Q_2 \\ \Delta H_3 \\ \Delta Q_3 \\ \Delta H_4 \\ \Delta Q_9 \\ \Delta Q_{10} \\ \Delta Q_{11} \\ \Delta H_5 \\ \Delta Q_5 \\ \Delta H_6 \\ \Delta Q_6 \\ \Delta H_7 \\ \Delta Q_7 \\ \Delta H_8 \\ \Delta Q_8 \end{bmatrix}
=
\begin{bmatrix} RHS_{H1} \\ RHS_{Q1} \\ RHS_{H2} \\ RHS_{Q2} \\ RHS_{H3} \\ RHS_{Q3} \\ RHS_{H4} \\ RHS_{Q9} \\ RHS_{Q10} \\ RHS_{Q11} \\ RHS_{H5} \\ RHS_{Q5} \\ RHS_{H6} \\ RHS_{Q6} \\ RHS_{H7} \\ RHS_{Q7} \\ RHS_{H8} \\ RHS_{Q8} \end{bmatrix} \tag{4}
$$

where ΔH_i and ΔQ_i = increments of head and flow at location i during Δt; ΔQ_9 represents flow at downstream end of link 3-4; and ΔQ_{10} and ΔQ_{11} = flows at upstream end of links 4-5 and 4-7, respectively. Using the superlink algorithm with the staggered grid implicit scheme, a sparse matrix with an order of 4, instead of the order of 18, is formulated. This example shows that the reduction of the order of the sparse matrix using the superlink algorithm could be substantial.

The superlink algorithm with the staggered grid, implicit discretization scheme outlined before is developed in detail in the following sections. All nonlinear coefficients for the variables duirng t–$t + \Delta t$ are linearized based on the solutions at time t in the following development.

Discretization of Momentum Equation

According to the staggered grid setup, the discretized momentum equation for link i in superlink k can be derived by discretizing (2) over link i, shown in Fig. 3(b)

$$
(Q_{ik}^{t+\Delta t} - Q_{ik}^{t})\frac{\Delta x_{ik}}{\Delta t} + u_{I+1k}Q_{I+1k}^{t+\Delta t} - u_{Ik}Q_{Ik}^{t+\Delta t}
$$

$$
+ gA_{ik}(S_{fik} + S_{Lik})\Delta x_{ik} = gA_{ik}S_{0ik}\Delta x_{ik} + gA_{ik}(h_{Ik}^{t+\Delta t} - h_{I+1k}^{t+\Delta t}) \tag{5}
$$

where subscript i = link number; I = node number; and subscript k = superlink sequential number. The variables without a superscript indicate that they are corresponding to time t. The superscript defined here is used throughout the development.

The Manning's equation is used to describe the frictional head loss

$$
S_{fik} = \frac{n_{ik}^2|Q_{ik}^t|Q_{ik}^{t+\Delta t}}{A_{ik}^2R_{ik}^{4/3}} \tag{6}
$$

where n_{ik} = Manning's coefficient; and R_{ik} = hydraulic radius. The local head loss slope s_{Lik} is derived from a general discharge equation

$$
Q_{ik} = C_{ik}A_{cik}\sqrt{g(H_{Ik} - H_{I+1k})} \tag{7}
$$

or, in linearized form

$$
S_{Lik} = \frac{H_{Ik}^{t+\Delta t} - H_{I+1k}^{t+\Delta t}}{\Delta x_{ik}} = \frac{|Q_{ik}^t|Q_{ik}^{t+\Delta t}}{gC_{ik}^2A_{cik}^2\Delta x_{ik}} \tag{8}
$$

where C_{ik} = discharge coefficient; and A_{cik} = flow cross-sectional area at location of control structure in link i. Velocities at nodes $I + 1$ and I are based on the linear interpolation between two links connected to the node as follows:

$$
u_{I+1k} = \frac{\Delta x_{ik}u_{i+1k} + \Delta x_{i+1k}u_{ik}}{\Delta x_{ik} + \Delta x_{i+1k}} \tag{9}
$$

$$
u_{Ik} = \frac{\Delta x_{ik}u_{i-1k} + \Delta x_{i-1k}u_{ik}}{\Delta x_{ik} + \Delta x_{i-1k}} \tag{10}
$$

Introducing (6), (8), (9), and (10) to (5), and collecting and rearranging the terms lead to the following discretized momentum equation for link i:

$$
a_{ik}Q_{i-1k}^{t+\Delta t} + b_{ik}Q_{ik}^{t+\Delta t} + c_{ik}Q_{i+1k}^{t+\Delta t} = P_{ik} + gA_{ik}(h_{Ik}^{t+\Delta t} - h_{I+1k}^{t+\Delta t}) \tag{11}
$$

where $a_{ik} = -\max(u_{Ik}, 0)$ and $c_{ik} = -\max(-u_{I+1k}, 0)$ are determined by upwind scheme for convection term (Patankar 1980)

$$
b_{ik} = \frac{\Delta x_{ik}}{\Delta t} + \frac{gn_{ik}^2|Q_{ik}^t|\Delta x_{ik}}{A_{ik}R_{ik}^{4/3}} + \frac{A_{ik}|Q_{ik}^t|}{A_{cik}^2C_{ik}^2} - a_{ik} - c_{ik} \tag{12}
$$

and

$$
P_{ik} = Q_{ik}\frac{\Delta x_{ik}}{\Delta t} + gA_{ik}S_{0ik}\Delta x_{ik} \tag{13}
$$

Discretization of Continuity Equation

The control volume at node I is shown in Fig. 3(c). The following equation is derived by discretizing (1) over the control volume:

$$
Q_{ik}^{t+\Delta t} - Q_{i-1k}^{t+\Delta t} + \left(\frac{B_{ik}\Delta x_{ik}}{2} + \frac{B_{i-1k}\Delta x_{i-1k}}{2} + A_{SIk}\right)
$$

$$
\cdot\frac{h_{Ik}^{t+\Delta t} - h_{Ik}^{t}}{\Delta t} = Q_{0Ik} \tag{14}
$$

where Q_{0Ik} = lateral flow rate to node I during Δt; B_{ik} and B_{i-1k} = top widths for links i and $i - 1$, respectively; and A_{SIk} = surface area of manhole attached to node I. By defining

$$
E_{Ik} = \left(\frac{B_{ik}\Delta x_{ik}}{2} + \frac{B_{i-1k}\Delta x_{i-1k}}{2} + A_{SIk}\right)\Big/\Delta t \tag{15}
$$

and

$$
D_{Ik} = Q_{0Ik} + \left(\frac{B_{ik}\Delta x_{ik}}{2} + \frac{B_{i-1k}\Delta x_{i-1k}}{2} + A_{SIk}\right)\frac{h_{Ik}^t}{\Delta t} \tag{16}
$$

the discretized continuity equation for node I is written as

$$
Q_{ik}^{t+\Delta t} - Q_{i-1k}^{t+\Delta t} + E_{Ik}h_{Ik}^{t+\Delta t} = D_{Ik}. \tag{17}
$$

Internal Boundary Conditions

According to the definition discussed previously, any sewer/channel network system can be broken down into a collection of superlinks connected to a number of superjunctions. The flow equation at the upstream end of the superlinks can be expressed as

$$
Q_{uk} = C_{uk}A_{uk}\sqrt{g\Delta H_{uk}}; \quad k = 1, 2, \ldots NK \tag{18}
$$

where subscripts uk indicates upstream end of superlink k; NK = number of superlinks in system; and ΔH_{uk} = difference between head at attached superjunction and head at upstream end of superlink k. The head difference is defined as $\Delta H_{uk} = H_{Juk} - \text{Zinv}_{uk} - h_{uk}$, H_{Juk} = head at superjunction attached to up-

stream end of superlink k; $Zinv_{uk}$ and h_{uk} = invert elevation and depth at upstream end of superlink k.

Increment of flow at the upstream end of superlink k during time Δt is determined by

$$\Delta Q_{uk} = Q_{uk}^{t+\Delta t} - Q_{uk} = \frac{\partial Q_{uk}}{\partial A_{uk}} (A_{uk}^{t+\Delta t} - A_{uk}) + \frac{\partial Q_{uk}}{\partial (\Delta H_{uk})} (\Delta H_{uk}^{t+\Delta t} - \Delta H_{uk}) \quad (19)$$

Substituting (18) into (19) and taking the partial derivatives leads to the following linearized upstream boundary condition for superlink k:

$$h_{uk}^{t+\Delta t} = \kappa_{uk} Q_{uk}^{t+\Delta t} + \lambda_{uk} H_{Juk}^{t+\Delta t} + \mu_{uk}; \quad k = 1, 2, \ldots NK \quad (20)$$

in which

$$\kappa_{uk} = \frac{2A_{uk}\Delta H_{uk}}{Q_{uk}(2\Delta H_{uk} B_{uk} - A_{uk})} \quad (21)$$

$$\lambda_{uk} = -\frac{A_{uk}}{2\Delta H_{uk} B_{uk} - A_{uk}} \quad (22)$$

$$\mu_{uk} = \frac{A_{uk}(H_{Juk} - h_{uk})}{2\Delta H_{uk} B_{uk} - A_{uk}} \quad (23)$$

Similarly, the linearized downstream boundary condition of the superlinks can be expressed as

$$h_{dk}^{t+\Delta t} = \kappa_{dk} Q_{dk}^{t+\Delta t} + \lambda_{dk} H_{Jdk}^{t+\Delta t} + \mu_{dk}; \quad k = 1, 2, \ldots NK \quad (24)$$

in which

$$\kappa_{dk} = \frac{2A_{dk}\Delta H_{dk}}{Q_{dk}(2\Delta H_{dk} B_{dk} + A_{dk})} \quad (25)$$

$$\lambda_{dk} = \frac{A_{dk}}{2\Delta H_{dk} B_{dk} + A_{dk}} \quad (26)$$

$$\mu_{dk} = \frac{A_{dk}(h_{dk} - H_{Jdk})}{(2\Delta H_{dk} B_{dk} + A_{dk})} \quad (27)$$

where subscript dk indicates downstream end of superlink k; and ΔH_{dk} = difference between head at upstream end of superlink k and head at attached superjunction. The head differences is defined as $\Delta H_{dk} = Zinv_{dk} + h_{dk} - H_{Jdk}$, where H_{Jdk} = head at superjunction attached to downstream end of superlink k; and $Zinv_{dk}$ and h_{dk} = invert elevation and depth at downstream end of superlink k.

Construction of Sparse Matrix Equation

Considering the discretized continuity and momentum equations [(11) and (17)], a pair of recurrence relations are developed that relate flows and heads at both ends of a superlink. Details of the development are presented in Appendix I. Once the superlink recurrence relations are established, the sparse matrix equation for flow and head at time $t + \Delta t$ throughout the sewer/channel network system can be constructed.

If there are M superjunctions in the system, the question is how to determine the head at each of the superjunctions. Assuming that there are NN internal superjunctions where the head is to be determined and that there are M-NN superjunctions attached to stage boundary conditions, the continuity equation for the NN internal superjunctions can be constructed as

$$\sum_{l=1}^{NBd_J} Q_{dk_l}^{t+\Delta t} - \sum_{m=1}^{NBu_J} Q_{uk_m}^{t+\Delta t} + Q_{0J} = \frac{A_{SJ}(H_J^{t+\Delta t} - H_J)}{\Delta t}; \quad J = 1, 2, \ldots NN \quad (28)$$

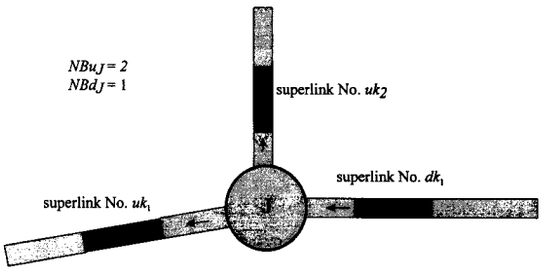

FIG. 5. Typical Superjunction Setup

where A_{SJ} = water-surface area of superjunction J; Q_{0J} = lateral flow to superjunction J; NBu_J = number of superlinks with its upstream end attached to superjunction J; NBd_J = number of superlinks with its downstream and attached to superjunction J; subscript k_m ($m = 1, \ldots NBu_J$) for Q_u = superlink sequential number with its upstream end attached to superjunction J; and k_l ($l = 1, \ldots NBd_J$) for Q_d = superlink sequential number with its downstream end attached to superjunction J. Fig. 5 shows the connectivity of a typical superjunction.

Given the head at the M-NN superjunctions where the stage boundary conditions are attached, the heads at the NN internal superjunctions can be solved if the flows from and to each superjunction are known or can be expressed in terms of the heads at the adjacent superjunctions.

According to recurrence relations (65) and (66) developed in Appendix I, the flow at each end of a superlink is expressed as a linear combination of heads at both ends of the superlink. The coefficients of the recurrence relations depend only on the system variables at time t. Introducing (65) for the upstream flows and (66) for the downstream flows in (28) and considering the connectivity of the superlinks, the following set of equations is developed:

$$F_{J,J} H_J^{t+\Delta t} + \sum_{l=1}^{NBd_J} \Phi_{J,Juk_l} H_{Juk_l}^{t+\Delta t} + \sum_{m=1}^{NBu_J} \Psi_{J,Jdk_m} H_{Jdk_m}^{t+\Delta t} = G_J; \quad J = 1, 2, \ldots M - NN \quad (29)$$

in which

$$F_{J,J} = \frac{A_{SJ}}{\Delta t} - \sum_{l=1}^{NBd_J} \beta_{dk_l} + \sum_{m=1}^{NBu_J} \alpha_{uk_m} \quad (30)$$

$$\Phi_{J,Juk_l} = -\alpha_{dk_l}; \quad l = 1, 2, \ldots NBD_J \quad (31)$$

$$\Psi_{J,Jdk_m} = \beta_{uk_m}; \quad m = 1, 2, \ldots NBu_J \quad (32)$$

and

$$G_J = \frac{A_{SJ}}{\Delta t} H_J + Q_{0J} + \sum_{l=1}^{NBd_J} \chi_{uk_l} - \sum_{m=1}^{NBu_J} \chi_{dk_m} \quad (33)$$

where Juk_l = sequential number of superjunctions at downstream end of superlink k_l; and Jdk_m = sequential number of superjunctions at upstream end of superlink k_m. The coefficients α, β, and χ are determined in Appendix I. As can be seen from the development, the other end of the superlink is attached to superjunction J; i.e., $Jdk_l = Juk_m = J$, ($l = 1, 2, \ldots NBu_J$, $m = 1, 2, \ldots NBd_J$).

The stage boundary conditions can be expressed as

$$H_J^{t+\Delta t} = H_{J\,\text{given}}; \quad J = M - NN + 1, \ldots M \quad (34)$$

The sparse matrix formulated from the NN equations in (29) and the M-NN boundary conditions in (34) has an order of M. The equation number and the superjunction number are used as the row and column numbers for each of the coefficients, respectively. For example, for the Jth equation represented by (29), $F_{J,J}$ is the diagonal element that represents the coefficients at row J and column J in the matrix. The coefficients Φ_{J,Juk_l} ($l = 1, 2, \ldots NBd_J$), and Ψ_{J,Jud_m} ($m = 1, 2, \ldots NBu_J$)

are off-diagonal in the sparse matrix. In the $M \times M$ matrix, J is the row number and Juk_l and Jdk_m are the column numbers of the corresponding coefficient. G_J is the right-hand side of the Jth equation. The diagonal element for the Jth equation represented by (34) is unity, and there is no off-diagonal element in the equation. The right-hand side of the equation is the given stage at superjunction J.

Solving Procedure

Based on the development of the algorithm and the numerical scheme, the following steps are summarized to solve flows and heads in a network system for one time step of computation.

1. Calculate a_{ik}, b_{ik}, c_{ik}, and P_{Ik} in (11) for each link in superlink k. Also calculate D_{Ik} and E_{Ik} in (17) for each node in superlink k.
2. Calculate coefficients U_{Ik}, V_{Ik}, and W_{Ik} for $I = 1-Nk$ using (45), (46), and (47) starting with (38), (39), and (40).
3. Calculate coefficients X_{Ik}, Y_{Ik}, and Z_{Ik} for $I = Nk-1$ to using (59), (60), and (61) starting with (52), (53), and (54).
4. Calculate κ_{uk}, λ_{uk}, μ_{uk}, κ_{dk}, λ_{dk}, and μ_{dk} using (21), (22), (23), (25), (26), and (27).
5. Calculate coefficients α_{uk}, β_{uk}, χ_{uk}, α_{dk}, β_{dk}, and χ_{uk} using (67), (68), (69), (70), (71), and (72).
6. Go through the procedure from steps 1–4 for all of the NK superlinks in the system.
7. Calculate $F_{J,J}$; $\Phi_{J,Juk}$; $\Psi_{J,Jdk}$; and G_J for each of the NN internal superjunctions using (30), (31), (32), and (33). Set $F_{J,J}$ equal to unity and G_J equal to the given head for the M-NN boundary superjunctions based on (34). This step determines the sparse matrix coefficients and the right-hand side vector.
8. Solve the $M \times M$ sparse matrix equation determined in step 7 to get heads at each of the superjunctions.
9. Calculate the flow at each end of the superlinks using (65) and (66) based on the solution of the sparse matrix equation.
10. Solve (44) and (58) for a detailed solution of flow in all the links and of depth at all the nodes in each superlink.

Once the flow and depth at time $t + \Delta t$ are solved, the solution is used as the initial condition for the next time step. Going through steps 1–10 repeatedly leads to the solution throughout the entire simulation period.

NUMERICAL TESTS

Numerical tests were carried out to examine the setup, speed, stability, and accuracy of the model. A series of tests were designed to examine the model performance with respect to stability and accuracy under the combined effects of backwater and storm flow in a looped network system. A trial network system shown in Fig. 6 was used for the tests under the inflow and stage boundary conditions defined in Fig. 7. There was no base flow imposed on the system so that the numerical experiments could be carried out for a situation unfavorable to numerical computation when dry pipes experience a reverse flow due to the rising downstream stage. Fig. 8 shows the simulation results of the head at junctions and the flow in conduits during the 10 h simulation.

The simulation started with a dry system as an initial condition; i.e., flows through each conduit were zero and heads at each junction were equal to the invert level. As shown in Fig. 8, the inflows at junctions **A** and **C** were zero in the first

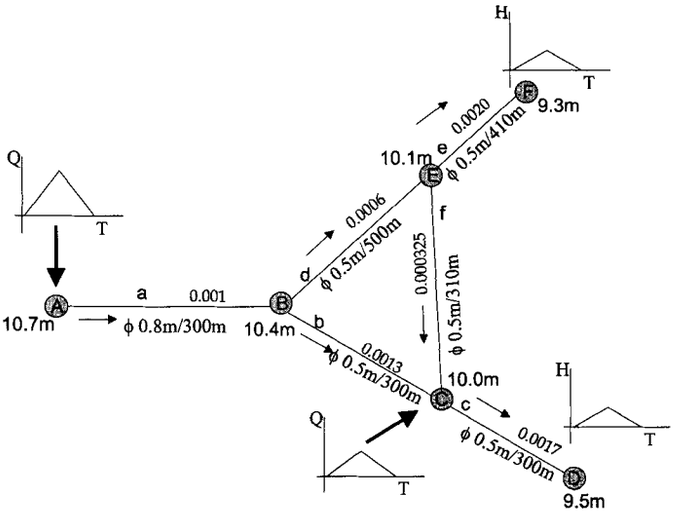

FIG. 6. Sewer Network System for Numerical Tests

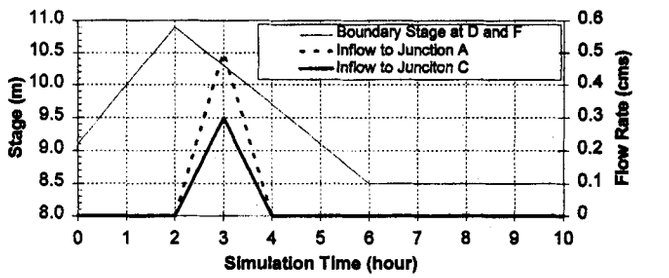

FIG. 7. Inflow and Downstream Stage Boundary Conditions for Numerical Tests

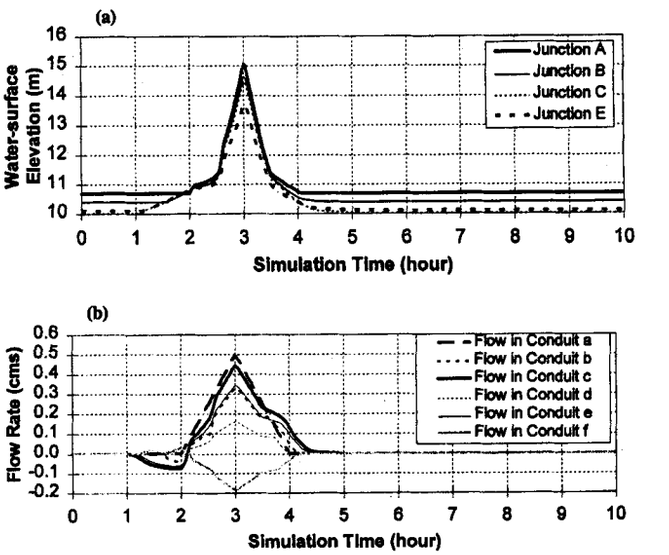

FIG. 8. Simulated Head and Flow in System: (a) Simulated Water-Surface Elevation at Junctions; (b) Simulated Flow in Conduits

2 h of simulation. The stages at the downstream junctions **D** and **F** were lower than the invert elevation at junctions **E** and **C** in first hour of the simulation. As a result, there was no flow through any conduits during the hour. In the second hour, however, the downstream stage started to get higher than the invert elevation at junctions **C**, **E**, **B**, and **A**, causing a small amount of negative flow through conduits **c**, **e**, **b**, and **d**. The reverse flow due to the rising downstream stage partially filled the system at the end of the 2 h simulation. Between 2 and 4 h of the simulation, inflows were applied to junctions **A** and

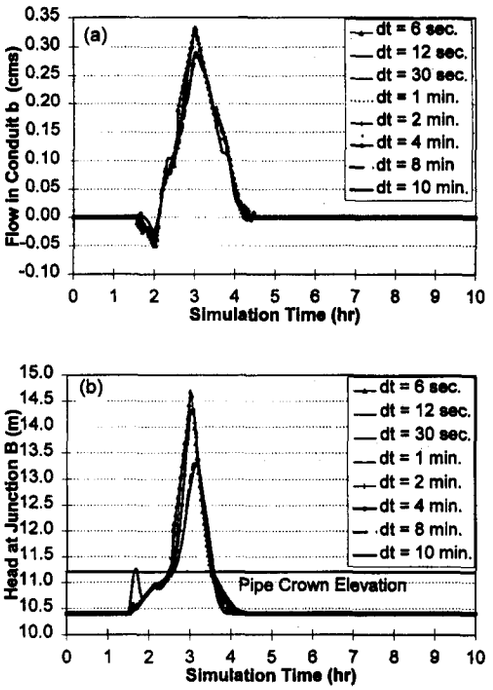

FIG. 9. Simulation Results for Time Grid Test

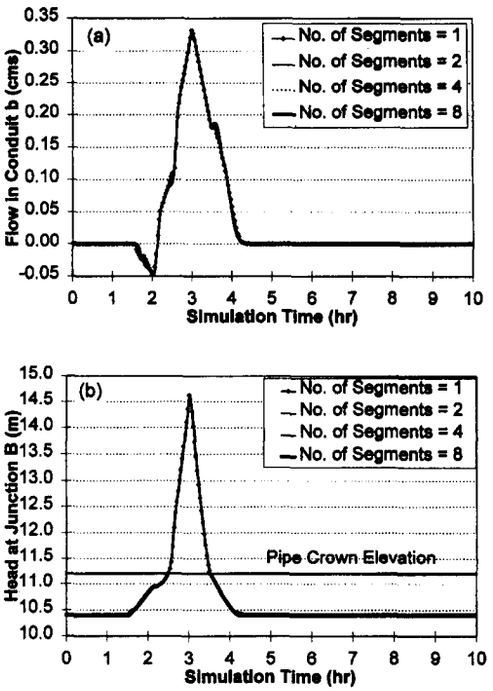

FIG. 10. Simulation Results for Space Grid test

C while the downstream stage was declining. The system started to drain water through downstream junctions **D** and **F**, indicated by the positive flow through conduits **c** and **e** [Fig. 8(b)]. The water level in the system was backed up and the system was obviously surcharged during this period. The head at junction **C** was higher than that at junction **E**, causing negative flow through conduit **f**. After 4 h of simulation, there was no inflow to the system and the downstream stage was declining to the level below the lowest location in the system. The water volume was drained off completely and the system remained dry during the rest of the simulation.

A series of simulations under the same conditions were carried out using different time steps. A comparison of the simulations using different time steps ranging from 6 to 600 s was made. The simulated flow in conduit **b** and the head at junction **B** were plotted in Fig. 9. The simulation with a time step of 600 s shows a symptom of instability, as can be seen in Fig. 9(b). It indicates that the time steps above 600 s may give unreliable results for the test case. The comparison indicates that there is a negligible difference between the solutions for the time steps ranging from 6 to 120 s. The difference becomes more and more significant as the time step gets bigger, suggesting that the effects of nonlinearity and numerical diffusion may become distinguishable at bigger time steps.

The simulated flows and heads with a different number of segments to the conduits were also compared as a space grid test. Conduits **a**, **b**, **c**, **d**, **e**, and **f** as shown in Fig. 6 were segmented into two, four, and eight links and were compared with the simulation results with no segmentation of the conduits. The simulated flow in conduit **b** and the head at junction **B** for different space grids are almost identical, as shown in Fig. 10. The results indicate that segmenting a conduit may not have a significant effect on the accuracy of the computation in the range tested.

The results of the tests suggest that the model can give consistent simulation results under different time and space grids in the range tested. It also indicates that the model is robust even under conditions unfavorable to the stability of computation, such as the situation when reverse flow is applied to a dry sewer network system.

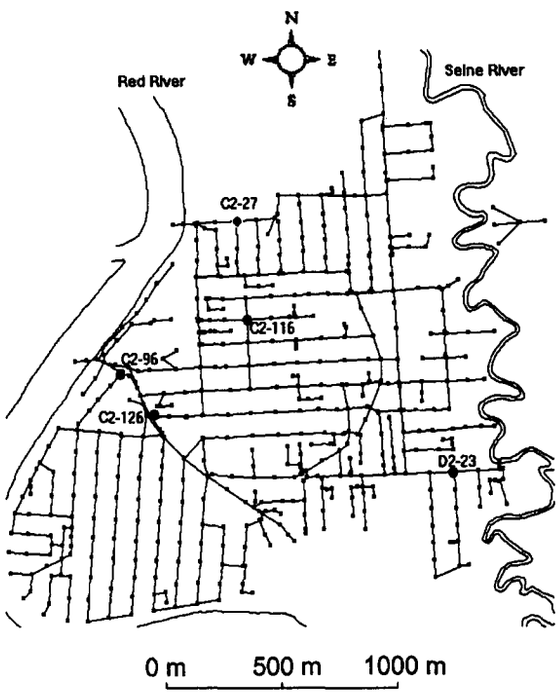

FIG. 11. Map of System for Model Verification

VERIFICATION

The SUPERLINK model was used to simulate the flow through a subset of the city of Winnipeg, Canada, sewer system to verify the applicability and reliability of the model under a variety of sewer network configurations and flow conditions. The system covers the 303 ha total Marion and Despins combined sewer districts located near central Winnipeg. The area is bounded on the west and south by the Red River and on the east by the Seine River. Fig. 11 shows the layout of the network system. There are 547 nodes and 592 links in the highly looped network system, grouped into 283 superlinks and 232 superjunctions in the computation. An inflow hydrograph corresponding to a 5 yr return period, gen-

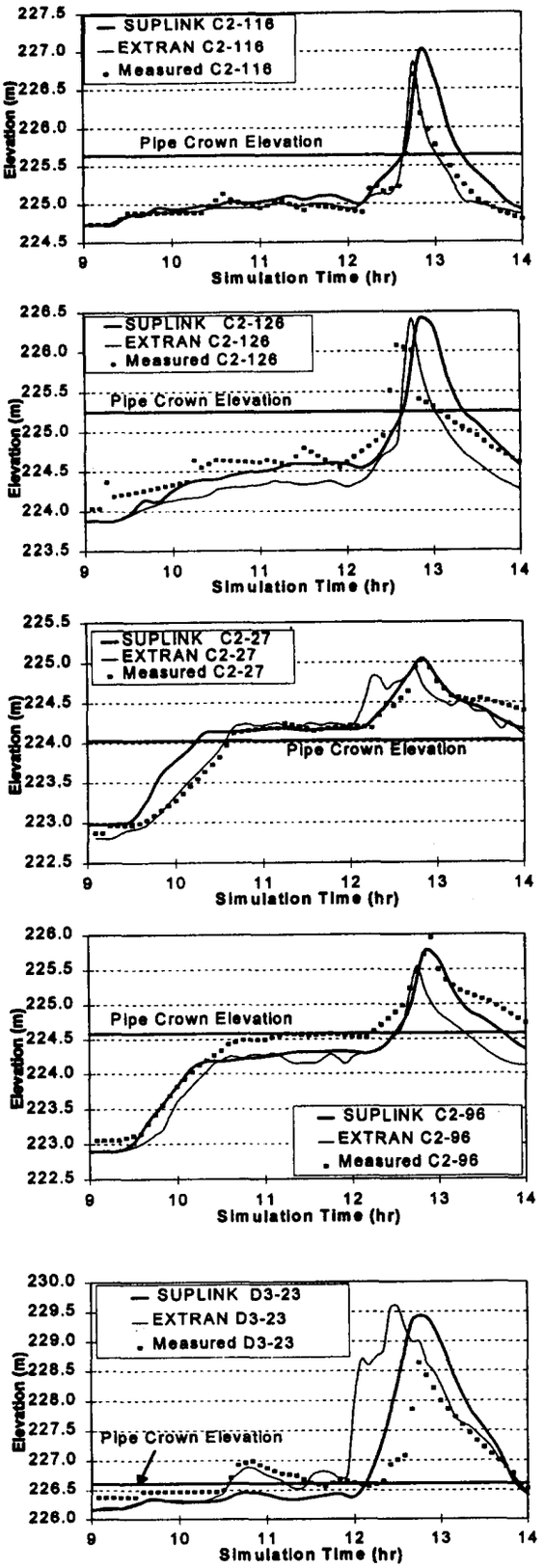

FIG. 12. Comparison between Measured and Simulated Results

erated from the SWMM RUNOFF model based on the rainfall record during July 24, 1993, is used for a 5 h simulation.

A mass balance check of the flow volume over the system is summarized to evaluate the model. Each inflow hydrograph is integrated over the 5 h period, and is compared with the total outflow volume and the net volume increment in the system over the period. The total water balance calculation gives an error of 0.32% for the 5 h simulation. The computation results of water surface elevation were compared with the measured data during the simulation period, as shown in Fig. 12. The SWMM EXTRAN model using the same network links and nodes under the same inflow and downstream stage boundary conditions was also plotted for comparison. In fact, the SWMM EXTRAN data file for the network was directly used for the SUPERLINK model simulation. The locations for the comparisons are indicated in Fig. 11. Measured water surface elevations show that the system was surcharged during the storm.

To evaluate the results, one should bear in mind that there are many factors beyond the hydraulic model that affect the accuracy of the prediction. Model simulations rely on the inflows, which were predicted using the SWMM RUNOFF model according to the rainfall record. In reality, the inflow is much more complicated and very difficult to predict accurately. The flow to the system during the storm depends mainly on inflow, infiltration, and exfiltration. Each component of flow is affected by many factors, such as the soil moisture, ground surface pavement conditions, ground-water table, and the maintenance conditions in each pipe. The inflow also depends on sanitary sewerage supply. These factors create uncertainties in predicting the flow hydrograph, making it difficult to evaluate the accuracy of the prediction from the hydraulic model. Under the shadow of these uncertainties, the comparison shows that the model results reasonably agree with the field measurement in both nonsurcharge and surcharge conditions.

The run time on an IBM compatible 486-66 MHz computer was 55 s for the 5 h simulation with a time step of 60 s. The run time on a per-pipe, per-hour basis is plotted in Fig. 13 with the time step ranging from 1 s to 480 s. The EXTRAN simulation statistics of speed using the same computer are also plotted as a reference. The EXTRAN model failed to simulate when the time step exceeded 7 s. The SUPERLINK model gave stable simulation results for the time step up to 8 min.

As is shown in Fig. 13, the SUPERLINK model benefits from the bigger time steps in reducing the computation effort, in addition to the gain of two to three times the computational speed compared to the same time step below 7 s. The desired speed of the model simulation makes it possible for applications of long-term simulation and real-time control for large looped systems.

CONCLUSIONS

An algorithm, the SUPERLINK algorithm, with a staggered-grid implicit scheme for hydrodynamic simulation of sewer/channel systems is presented. The discretized form of the continuity and momentum equations is applied to the space dimension with a staggered grid setup to improve the stability of the computation. The flows and depths in a network system are solved in two steps using the SUPERLINK algorithm. First, solve a condensed matrix equation, which is based on the solution of a previous time step, for the heads at super-

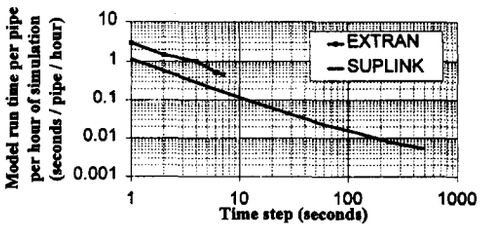

FIG. 13. Model Run Time for EXTRAN and SUPERLINK

junctions. Second, solve the recurrence equations of superlinks for flows in links and depths at nodes, based on the solution of the sparse matrix equation given in step 1.

A computer model, SUPERLINK, for looped sewer/channel systems, is developed based on the SUPERLINK algorithm. The applicability and stability of the model are demonstrated through numerical tests. The results of the simulations using different grid sizes in the time and space dimensions are consistent.

The SUPERLINK model is used to simulate the flow through a large sewer system, which experienced both free surface and surcharged conditions, for the city of Winnipeg. Results of the simulation are shown to be in reasonable agreement with measurements and with the simulation results using the SWMM EXTRAN model. This example, together with the numerical tests, demonstrated that the accuracy and stability of the SUPERLINK model are satisfactory. The desirable computation speed of the SUPERLINK model particularly makes the model suitable for long-term simulations and real-time control applications.

APPENDIX I. RECURRENCE RELATIONS FOR SUPERLINK

Considering the upstream end of superlink k shown in Fig. 4(a), (17) for node 2 is expressed as the following:

$$Q_{2k}^{t+\Delta t} - Q_{1k}^{t+\Delta t} + E_{2k}h_{2k}^{t+\Delta t} = D_{2k} \tag{35}$$

Eq. (11) for link 1 is expressed as

$$a_{1k}Q_{0k}^{t+\Delta t} + b_{1k}Q_{1k}^{t+\Delta t} + c_{1k}Q_{2k}^{t+\Delta t} = P_{1k} + gA_{1k}(h_{1k}^{t+\Delta t} - h_{2k}^{t+\Delta t}) \tag{36}$$

Assuming $Q_{0k}^{t+\Delta t} = Q_{1k}^{t+\Delta t}$ at the upstream end of the superlink and combining (35) and (36) yields

$$(a_{1k} + b_{1k} + c_{1k})Q_{1k}^{t+\Delta t} = (E_{2k}c_{1k} - gA_{1k})h_{2k}^{t+\Delta t} + P_{1k} - D_{2k}c_{1k} + gA_{1k}h_{1k}^{t+\Delta t} \tag{37}$$

By defining

$$U_{1k} = \frac{E_{2k}c_{1k} - gA_{1k}}{T_{1k}} \tag{38}$$

$$V_{1k} = \frac{P_{1k} - D_{2k}c_{1k}}{T_{1k}} \tag{39}$$

$$W_{1k} = \frac{gA_{1k}}{T_{1k}} \tag{40}$$

and

$$T_{1k} = a_{1k} + b_{1k} + c_{1k} \tag{41}$$

we have

$$Q_{1k}^{t+\Delta t} = U_{1k}h_{2k}^{t+\Delta t} + V_{1k} + W_{1k}h_{1k}^{t+\Delta t} \tag{42}$$

When the relationship at $I = 1$ is known, deriving the relationship at I from $I - 1$ will lead to all the recurrence relations between $I = 1$ and Nk. The recurrence relationship between $h_{1k}^{t+\Delta t}$, $h_{Ik}^{t+\Delta t}$, and $Q_{I-1k}^{t+\Delta t}$ may be written as

$$Q_{I-1k}^{t+\Delta t} = U_{I-1k}h_{Ik}^{t+\Delta t} + V_{I-1k} + W_{I-1k}h_{1k}^{t+\Delta t};$$
$$(i = I = 2, 3, \ldots Nk + 1;\ Nk > 2) \tag{43}$$

When $I = 2$, (43) becomes (42).

Combining (17) for nodes I and $I + 1$, (43), and (11) for link i in favor of $h_{I+1k}^{t+\Delta t}$ and $Q_{ik}^{t+\Delta t}$ yields

$$Q_{ik}^{t+\Delta t} = U_{Ik}h_{I+1k}^{t+\Delta t} + V_{Ik} + W_{Ik}h_{1k}^{t+\Delta t} \tag{44}$$

where

$$U_{Ik} = \frac{E_{I+1k}c_{ik} - gA_{ik}}{T_{ik}} \tag{45}$$

$$V_{Ik} = \frac{P_{ik} + a_{ik}D_{Ik} - D_{I+1k}c_{ik} - (gA_{ik} - E_{Ik}a_{ik})\dfrac{V_{I-1k} + D_{Ik}}{U_{I-1k} - E_{Ik}}}{T_{ik}} \tag{46}$$

$$W_{Ik} = -\frac{gA_{ik} - E_{Ik}a_{ik}}{(U_{I-1k} - E_{Ik})T_{ik}}W_{I-1k} \tag{47}$$

$$T_{ik} = \left(a_{ik} + b_{ik} + c_{ik} - \frac{gA_{ik} - E_{Ik}a_{ik}}{U_{I-1k} - E_{Ik}}\right) \tag{48}$$

Given the system conditions at time t, the coefficients U_{Ik}, V_{Ik}, and W_{Ik} for $I = 1-Nk$ can be determined using (45), (46), and (47) starting with (38), (39), and (40).

On the other hand, the continuity equation [(17)] for node Nk is expressed as the following:

$$Q_{nk}^{t+\Delta t} - Q_{nk-1}^{t+\Delta t} + E_{Nk}h_{Nk}^{t+\Delta t} = D_{Nk} \tag{49}$$

The momentum equation [(11)] for link nk is expressed as

$$a_{nk}Q_{nk-1}^{t+\Delta t} + b_{nk}Q_{nk}^{t+\Delta t} + c_{nk}Q_{nk+1}^{t+\Delta t} = P_{nk} + gA_{nk}(h_{Nk}^{t+\Delta t} - h_{Nk+1}^{t+\Delta t}) \tag{50}$$

Assuming $Q_{nk+1}^{t+\Delta t} = Q_{nk}^{t+\Delta t}$ at the downstream end of superlink k, and combining (49) and (50) yields

$$(a_{nk} + b_{nk} + c_{nk})Q_{nk}^{t+\Delta t} = (gA_{nk} - a_{nk}E_{Nk})h_{Nk}^{t+\Delta t} + P_{nk} + a_{nk}D_{Nk} - gA_{nk}h_{Nk+1}^{t+\Delta t} \tag{51}$$

By defining

$$X_{Nk} = \frac{(gA_{nk} - E_{Nk}a_{nk})}{O_{nk}} \tag{52}$$

$$Y_{NK} = \frac{P_{nk} + D_{Nk}a_{nk}}{O_{nk}} \tag{53}$$

$$Z_{Nk} = \frac{-gA_{nk}}{O_{nk}} \tag{54}$$

and

$$O_{nk} = (a_{nk} + b_{nk} + c_{nk}) \tag{55}$$

we have

$$Q_{nk}^{t+\Delta t} = X_{Nk}h_{Nk}^{t+\Delta t} + Y_{Nk} + Z_{Nk}h_{Nk+1}^{t+\Delta t} \tag{56}$$

Similarly, given the relationship at $I = Nk$, deriving the relationship at I from $I + 1$ will lead to all the recurrence relations from Nk to 1. The recurrence relation among h_{Nk+1}, h_{I+1k}, and Q_{i+1k} may be expressed as

$$Q_{i+1k}^{t+\Delta t} = X_{I+1k}h_{I+1k}^{t+\Delta t} + Y_{I+1k} + Z_{I+1k}h_{NK+1}^{t+\Delta t};$$
$$(i = I = 1, 2, \ldots nk - 1;\ Nk > 2) \tag{57}$$

Combining (17) for nodes I and $I + 1$, (57), and (11) for link i, in favor of h_{Ik} and Q_{ik}, yields

$$Q_{ik}^{t+\Delta t} = X_{Ik}h_{Ik}^{t+\Delta t} + Y_{Ik} + Z_{Ik}h_{Nk+1}^{t+\Delta t} \tag{58}$$

where

$$X_{Ik} = \frac{(gA_{ik} - E_{Ik}a_{ik})}{O_{ik}} \tag{59}$$

$$Y_{Ik} = \frac{P_{ik} + D_{Ik}a_{ik} - D_{I+1k}c_{ik} - (gA_{ik} - E_{I+1k}c_{ik})\dfrac{D_{I+1k} - Y_{I+1k}}{X_{I+1k} + E_{I+1k}}}{O_{ik}} \tag{60}$$

$$Z_{Ik} = \frac{(gA_{ik} - E_{I+1k}c_{ik})Z_{I+1k}}{(X_{I+1k} + E_{I+1k})O_{ik}} \tag{61}$$

and

$$O_{ik} = \left(a_{ik} + b_{ik} + c_{ik} + \frac{gA_{ik} - E_{I+1k}c_{ik}}{X_{I+1k} + E_{I+1k}}\right) \tag{62}$$

Using the given system conditions at time t, the coefficient X_{Ik}, Y_{Ik}, and Z_{Ik} for $I = Nk-1$ can be determined using (59), (60), and (61) starting with (52), (53), and (54).

The flows and the depths in any of the internal links and nodes in a superlink can be solved using (44) and (58) when flows at both ends of the superlink are given.

Deriving (58) for $I = 1$ and (44) for $I = Nk$, a set of equations for superlink k is written as

$$Q_{uk}^{t+\Delta t} = X_{1k}h_{uk}^{t+\Delta t} + Y_{1k} + Z_{1k}h_{dk}^{t+\Delta t} \tag{63a}$$

$$Q_{dk}^{t+\Delta t} = U_{Nk}h_{dk}^{t+\Delta t} + V_{Nk} + W_{Nk}h_{uk}^{t+\Delta t} \tag{63b}$$

where subscripts u and d refer to up- and downstream ends of superlink.

The linearized boundary conditions at the ends of superlink k are written as the following [refer to (20) and (24)]:

$$h_{uk}^{t+\Delta t} = \kappa_{uk}Q_{uk}^{t+\Delta t} + \lambda_{uk}H_{Juk}^{t+\Delta t} + \mu_{uk} \tag{64a}$$

$$h_{dk}^{t+\Delta t} = \kappa_{dk}Q_{dk}^{t+\Delta t} + \lambda_{kd}H_{Jdk}^{t+\Delta t} + \mu_{dk} \tag{64b}$$

Combining (63) and (64), eliminating $h_{uk}^{t+\Delta t}$ and $h_{dk}^{t+\Delta t}$, and collecting and rearranging the terms lead to the linear equations for the flow at both the upstream and downstream ends of superlink k

$$Q_{uk}^{t+\Delta t} = \alpha_{uk}H_{Juk}^{t+\Delta t} + \beta_{uk}H_{Jdk}^{t+\Delta t} + \chi_{uk} \tag{65}$$

$$Q_{dk}^{t+\Delta t} = \alpha_{dk}H_{Juk}^{t+\Delta t} + \beta_{dk}H_{Jdk}^{t+\Delta t} + \chi_{dk} \tag{66}$$

where α_{uk}, β_{uk}, χ_{dk}, β_{dk}, and χ_{dk} = coefficients written as

$$\alpha_{uk} = \frac{(1 - U_{Nk}\kappa_{dk})X_{1k}\lambda_{uk} + Z_{1k}\kappa_{dk}W_{Nk}\lambda_{uk}}{D_k^*} \tag{67}$$

$$\beta_{uk} = \frac{(1 - U_{Nk}\kappa_{dk})Z_{1k}\lambda_{dk} + Z_{1k}\kappa_{dk}U_{Nk}\lambda_{dk}}{D_k^*} \tag{68}$$

$$\chi_{uk} = [(1 - U_{Nk}\kappa_{dk})(X_{1k}\mu_{uk} + Y_{1k} + Z_{1k}\mu_{dk}) + Z_{1k}\kappa_{dk}(W_{Nk}\mu_{uk} + V_{Nk} + U_{Nk}\mu_{dk})/D_k^*] \tag{69}$$

$$\alpha_{dk} = \frac{(1 - X_{1k}\kappa_{uk})W_{Nk}\lambda_{uk} + X_{1k}\kappa_{uk}W_{Nk}\lambda_{uk}}{D_k^*} \tag{70}$$

$$\beta_{dk} = \frac{(1 - X_{1k}\kappa_{uk})U_{Nk}\lambda_{dk} + W_{Nk}\kappa_{uk}Z_{1k}\lambda_{dk}}{D_k^*} \tag{71}$$

and

$$\chi_{dk} = [(1 - X_{1k}\kappa_{uk})(W_{Nk}\mu_{uk} + V_{Nk} + U_{Nk}\mu_{dk}) + W_{Nk}\kappa_{uk}(X_{1k}\mu_{uk} + Y_{1k} + Z_{1k}\mu_{dk})/D_k^*] \tag{72}$$

in which

$$D_k^* = \begin{vmatrix} 1 - X_{1k}\kappa_{uk} & -Z_{1k}\kappa_{dk} \\ -W_{nk}\kappa_{uk} & 1 - U_{Nk}\kappa_{dk} \end{vmatrix}. \tag{73}$$

ACKNOWLEDGMENT

This work was conducted when the writer was working with Reid Crowther Consulting Inc.

APPENDIX II. REFERENCES

Abbot, M. B. (1982). "A model system for design and operation of storm-sewer networks." *Engineering application of computational hydraulics*, M. B. Abbot and J. A. Cunge, eds., Vol. 1, Homage to Alexandra Preissmann, Pitman Advanced Publishing Program, Boston, 11–36.

Amein, M. (1968). "An implicit method for natural flood routing." *Water Resour. Res.*, 4(4), 719–726.

Fread, D. L. (1973). "Technique for implicit dynamic routine in rivers with tributaries." *Water Resour. Res.*, (4), 918–926.

Joliffe, I. B. (1984). "Computation of dynamic waves in channel networks." *J. Hydr. Engrg.*, ASCE, 110(10), 1358–1369.

Nguyen, Q. K., and Kawano, H. (1995). "Simultaneous solution for flood routing in channel networks." *J. Hydr. Engrg.*, ASCE, 121(10), 744–750.

Patankar, S. V. (1980). *Numerical heat transfer and fluid flow.* Hemisphere Publishing Corp., McGraw-Hill Book Co., Inc., New York, N.Y.

Price, R. K. (1974). "Comparison of four numerical methods for flood routing." *J. Hydr. Div.*, ASCE, 100(7), 879–899.

Roesner, L. A., Aldrich, J. A., and Dickinson, R. E. (1988). *Storm water management model user's manual version 4: EXTRAN addendum 1 EXTRAN.* Cooperative Agreement CR-811607, U.S. Envir. Protection Agency, Cincinnati, Ohio.

Strelkoff, T. (1973). "Numerical solution of the St. Venant equations." *J. Hydr. Div.*, ASCE, 96(1), 223–252.

APPENDIX III. NOTATION

The following symbols are used in this paper:

A, A_c = cross-sectional area of flow;
A_s = water surface area of junction;
a, b, c = coefficients;
B = top width;
C = discharge coefficient of control structure;
D, D^*, E, F, G = coefficients;
g = gravitational acceleration;
H = head;
h = depth;
I = index for nodes;
i = index for links;
J, Juk, Jdk = index for superjunctions;
k, uk, dk = index for superlinks;
M = total number of superjunctions;
NBd_J = number of superlinks with downstream end connected to junction J;
NBU_J = number of superlinks with upstream end connected to junction J;
NK = total number of superlinks;
Nk = total number of nodes in superlink k;
NN = total number of stage boundary conditions;
n = Manning's roughness coefficient;
nk = index for total number of links in superlink k;
O, P = coefficients;
Q_0, q_0 = lateral flow;
R = hydraulic radius;
RHS = right-hand side of equation;
S_f = friction head loss slope;
S_L = local head loss slope;
S_0 = bed slope;
T = coefficient;
t = time;
U, V, W = coefficients;
u = velocity;
X, Y, Z = coefficients;
x = distance;
Zinv = invert elevation;
α, β, χ = coefficients;
κ, λ, μ = coefficients;
Φ = coefficient; and
ψ = coefficient.